SPE 129904

Analytical Formulae for In-Situ Combustion

A.A. Mailybaev, Institute of Mechanics, Moscow State Lomonosov University, J. Bruining, SPE, Delft University of Technology, D. Marchesin, Instituto Nacional de Matemática Pura e Aplicada, Rio de Janeiro

This paper was prepared for presentation at the 2010 SPE Improved Oil Recovery Symposium held in Tulsa, Oklahoma, USA, 24–28 April 2010.

Abstract

There is a renewed interest in using combustion to recover difficult oil. In spite of numerous experimental, numerical and analytical studies, the mechanisms for incomplete fuel combustion or oxygen consumption are not fully understood. Incomplete fuel combustion or oxygen consumption are indicators of sub-optimal process conditions and hazardous oxygen breakthrough in the production wells. This paper shows that these features emerge in a relatively simple 1-D model, where air is injected in a porous medium filled with inert gas, water and an oil mixture consisting of precoke, medium and light oil. Precoke is a component that is dissolved in the oil, but has essentially the same composition as coke. At high temperatures, precoke is converted to coke, which participates in high-temperature oxidation. At high temperatures, medium oil components are cracked releasing gaseous oil. Light oil components and water are vaporized. The model possesses an analytical solution, which was obtained by a method introduced by Zeldovich. This method entails that reaction can only occur in a very small temperature range, due to the highly non-linear nature of the Arrhenius factor. For a temperature below this range the reaction rate is too slow and for temperatures above this range the reacton rate is so fast that either the fuel or oxygen concentrations become zero. The model results show that there are two combustion regimes in which coke or oxygen is partially consumed. In one regime the reaction zone moves in front of the heat wave, whereas in the other regime the order of the waves is reversed. There are also two combustion regimes in which the coke and oxygen are completely consumed. Also here the reaction zone can move in front or at the back of the heat wave. Each combustion regime is described by a sequence of waves; we derive formulae for parameters in these waves. We analyse our formulae for typical in-situ combustion data and compare the results with numerical simulation.

Introduction

There is recent interest in developing methods to recover “difficult oil“. One of the options to recover medium viscosity oil, i.e., oil with a viscosity between 10^2 and 10^4 [cP], is the application of air injection (Castanier and Brigham 1997; Castanier and Brigham 2003; Kuhn and Koch 1953), leading to oil combustion. The most critical issue for oil combustion is incomplete consumption of oxygen, leading to possible hazardous conditions at the production well (Bowes and Thomas 1966). Another issue is extinction, which is related to incomplete fuel or oxygen consumption. Finally there are efficiency considerations, also tied up with incomplete consumption. Current methods to describe the process are either performing complex experiments or time consuming numerical simulations; what is missing is a quick method to explore a large sample of possible process conditions. Such a quick method can be obtained if one would sacrifice multi-dimensionality (2-D or 3-D) for the sake of resolving the non-linearities in the process. Until now, however, no analytical solutions have been published for 1-D in-situ combustion processes that involve cracking, solid fuel consumption and evaporation, mostly due to the high non-linearity of the Arrhenius factor. Even in 1-D this is not a trivial problem, because combustion, cracking, etc., occur in narrow regions, yielding a tough multi-scale problem (Gerritsen and Durlofsky 2005; Kristensen et al. 2007). For various combustion conditions, analytical studies of combustion waves in porous media containing solid fuel were performed in (Akkutlu and Yortsos 2003; Aldusin et al. 2006; Aldushin et al. 1996; Aldushin et al. 1997; Bruining et al. 2009; Byrne and Norbury 1997; Schult et al. 1998; Schult et al. 1996; Wahle et al. 2003). Periodic and other non-steady combustion regimes were investigated in (Bayliss and Matkowsky 1994; Matkowsky and Sivashynsky 1978). A wave structure analysis within a thin combustion zone is necessary. This represents the main mathematical difficulty of such studies. We expect that the model that includes cracking, solid fuel consumption and evaporation can reveal the various combustion regimes, i.e.,

conditions for which the reaction front is downstream or upstream of the heat wave and conditions for incomplete fuel or oxygen consumption. When sufficient water is injected the combustion wave is driven by the cooling rate caused by the cold water injection (Dietz and Weijdema 1968; Weijdema 1968), rather than by the fuel consumption rate; we do not consider this case.

A number of pioneering papers have built up our present understanding of the oil combustion process. Application of air injection is one of the oldest EOR techniques, see, e.g., United States Patents 1473348 (1923) and 2642943 (1953), but soon afterwards it became less important than steam injection and steam soak. However oil combustion as a recovery technique has provoked a steady stream of papers in the petroleum engineering literature. The essence of the process was already established by Ramey (1954). He proposed that the oxygen in the air burns the heavier components of oil (Abou Kassem et al. 1986; Akin et al. 2000; Kok and Karacan 2000; Lin et al. 1987; Lin et al. 1984) generating a heat wave leading to vaporization of lighter components that are produced.

In this paper, we analyze model that includes a three pseudo-component crude oil for in-situ combustion. The pseudo-components are distinguished according to the types of reaction in which they participate, viz., oxidation, cracking and vaporization. We approximate the combustion region in the whole solution as a sequence of waves traveling with constant speeds, separated by regions where the properties are almost homogeneous. For the time being we take the reservoir state ahead of the combustion/cracking/evaporation wave as known. Otherwise, one needs an extension of the present model to flow, condensation and slow oxidation reactions in the reservoir at relatively low temperatures, which is a separate problem. We use a concept introduced by Zeldovich for the analysis of combustion waves, derive explicit formulae for the dependent variables in these waves and classify possible combustion regimes. The essence of his idea is that combustion occurs in a very small temperature window. For temperatures that are too low, the Arrhenius factor shows that the reaction rates become too slow. For temperatures that are too high the reaction rate becomes so fast that the combustion mixture will become depleted of an essential reactant. Stability and accuracy of the analytical solution were checked against accurate simulations for representative problem parameters.

The structure of the paper is as follows. First we describe the model. Next, we discuss combustion regimes providing explicit conditions for each regime and parameters of combustion waves. Subsequently we give the results of numerical calculations with typical reservoir data for in-situ combustion. We end with the Conclusion. The Appendices provide some sketches of the calculations; a more detailed treatment can be found in Mailybaev et al. (2010).

Model

We study forward combustion when a gaseous oxidizer (air) is injected into a porous medium, e.g., a rock cylinder thermally insulated against lateral heat losses and filled with gas, some crude oil and water. We consider medium viscosity oil. The mobility of any components other than gas will be ignored, because it is assumed that the speed of the reaction wave exceeds substantially the speed of any liquids. We express the concentrations and reaction rates in mass per unit pore volume and mass per unit pore volume per unit time respectively.

The oil in the reservoir contains various components, viz. saturates, aromats, resins and asphaltenes. The heaviest components (asphaltenes) are converted into coke in the high temperature zone. We use the word precoke to denote these components. We disregard both the formation of gaseous components during this conversion process and the heat of reaction associated with the splitting (Abu Khamsin et al. 1988). Therefore, we will consider the precoke as well as its product (coke) as a single pseudo-component with carbon concentration n_h [kg/m^3]. The combustion of coke in the presence of oxygen gives rise to the highest temperatures present in the combustion process. It is called high-temperature oxidation (HTO). We model HTO as a single reaction

$$C + O_2 \to CO_2 . \tag{1}$$

The other components, viz., saturates, aromats and resins, are lumped into two pseudo-components, i.e., light and medium oil. The light components are vaporized ahead of the combustion zone. The concentration of the light oil is denoted by n_v [kg/m^3]. The average molar weight of the light oil pseudo-component is denoted by M_v [kg/mol]. If water is present, we lump it into the light oil component, because they vaporize in the same region. The concentration of the medium oil pseudo-component is denoted by n_c [kg/m^3]. As temperature increases, the medium oil cracks into various components, which are released as vapor, i.e., they do not form coke. The average molar weight of these vapor components is denoted by M_c [kg/mol].

The three pseudo-components (precoke/coke, medium and light oil) are distinguished according to the corresponding process: HTO, cracking and vaporization. Transport of oil by convection is disregarded as explained above. Therefore, it is possible to write the rate of change of oil concentrations in terms of the reaction rates W [kg/m^{3}s] as follows

$$\frac{\partial n_h}{\partial t} = -W_h, \quad \frac{\partial n_c}{\partial t} = -W_c, \quad \frac{\partial n_v}{\partial t} = -W_v. \tag{2}$$

The gas phase contains oxygen, gaseous oil, steam, combustion products (carbon dioxide) and initial inert gas. In some combustion regimes, oxygen may be present in the gas together with gaseous light oil, leading to an oxidation reaction. However, as we will see below, gaseous light oil appearing due to cracking or vaporization is immediately transported to colder zones where the oxidation rate is so small that it can be ignored. This is why we do not need to distinguish the different components of gaseous oil. In the gas composition, we will distinguish the mole fraction Y of oxygen and the remaining gas fraction $1-Y$ that consists of vaporized oil, steam, combustion products and the initial inert gas. The mass balance equations for the gas fractions, ignoring diffusion, are

$$\frac{\partial \varphi (1-Y)\rho}{\partial t} + \frac{\partial (\rho u - \rho u Y)}{\partial x} = \frac{W_h}{M_h} + \frac{W_c}{M_c} + \frac{W_v}{M_v}, \tag{3}$$

$$\frac{\partial \varphi Y \rho}{\partial t} + \frac{\partial \rho u Y}{\partial x} = -\frac{W_h}{M_h}, \tag{4}$$

where φ is the porosity, ρu is the molar gas flux, $\rho u Y$ is the molar oxygen flux, $\rho = P_{tot} / RT$ [mol/m^3] is the molar density of gas at the prevailing pressure P_{tot} [Pa], u [m/s] is the gaseous phase Darcy velocity, M_h = 0.012 [kg/mol] is the carbon molar mass. Pressure variations are assumed to be small, so we take $P_{tot} = const$. The sum of (3) and (4) gives the mass balance for the total gas

$$\frac{\partial \varphi \rho}{\partial t} + \frac{\partial \rho u}{\partial x} = \frac{W_c}{M_c} + \frac{W_v}{M_v}. \tag{5}$$

The W_h term cancels out as the coke oxidation reaction (1) produces no net gas. Since the gas speed u / φ is about 10^2 times larger than thermal or combustion waves speeds, the first (accumulation) terms in the left-hand sides of (3)-(5) are small and will be neglected from now on.

Neglecting heat losses, we write the heat equation as

$$\frac{\partial C_m T}{\partial t} + \frac{\partial c_g (T - T_{st}) \rho u}{\partial x} = \lambda \frac{\partial^2 T}{\partial x^2} + Q_h W_h - Q_c W_c - Q_v W_v. \tag{6}$$

Here T [K] is the temperature and T_{st} = 293.15K is our reference temperature, λ [W/mK] is the thermal conductivity of the porous medium, C_m [J/m^3 K] is the heat capacity per unit volume of the porous medium, which is taken approximately equal to the constant heat capacity of the rock. We disregard gas, water and oil heat capacities compared to rock heat capacity in the accumulation term, because in all cases of interest the amount of liquids is small. The gas heat capacity c_g [J/mol K] is taken approximately as $c_g \approx 3.5R$, ignoring small variations of the heat capacity among different gas components. The heats Q_h, Q_c, Q_v [J/kg] correspond to HTO reaction, cracking and vaporization of light oil/water. They are all positive, except in the rare cases when Q_c is negative.

Arrhenius' law and the assumption of a linear dependence on the fuel concentration and oxygen concentration lead to

$$W_h = K_h Y n_h \exp\left(\frac{-E_h}{RT}\right) \tag{7}$$

with activation energy E_h [J/mol] and frequency factor K_h [1/s] (Abu-Khamsin et al. 1986). They are used for the HTO reaction rate. We will not need an expression for the vaporization rate, because it affects only the internal structure of the condensation wave, which is not relevant here. For the cracking reaction rate, it is suggested by the same authors to use

$$W_c = K_c n_c \exp\left(\frac{-E_c}{RT}\right) \tag{8}$$

with activation energy E_c and frequency factor K_c. The variables to be found are the temperature T, the concentrations n_h, n_c, n_v, Y and the Darcy velocity u. All the coefficients in the equations C_m, c_g, λ, etc. are assumed to be constant. The molar flux of injected air is $(\rho u)_{inj}$. The injected oxygen flux is $(\rho u Y)_{inj}$, with an oxygen mole fraction Y_{inj}. Ignition occurs at the entrance of the reservoir and combustion propagates in the same direction as the injected air.

Combustion regimes

In this section we provide a quantitative analytical description for possible in-situ combustion regimes that have the form of sequences of waves traveling with constant speeds. Derivations of these formulae are given in the Appendices.

In-situ combustion generates a wide hot region, where the heat released in the HTO reaction is stored. However, the region where the HTO reaction takes place is very thin. It is conventional to distinguish between a reaction-leading combustion structure, where the HTO region is ahead of the hot zone, and a reaction-trailing structure, where the HTO region is behind of the hot zone (Wahle et al. 2003).

Reaction-leading structure

The reaction-leading structure is shown schematically in **Fig. 1**. It contains a reaction wave traveling with speed υ followed by a slower thermal wave, with speed (see, e.g., Bruining et al. 2009)

$$\upsilon_T = c_g \left(\rho u\right)_{inj} / C_m. \tag{9}$$

The hot zone between these waves contains only injected gas. The reaction wave contains several thin regions. In **Fig. 2**, there is a thin HTO region at the left, where coke oxidation occurs, with further to the right wider regions where cracking and vaporization occur. The presence of a hot zone containing oxygen behind the reaction wave ensures that all coke is consumed in the HTO reaction. Oxygen consumption is not necessarily complete, so the HTO reaction is coke controlled. Ahead of the reaction wave the temperature drops to the vapor zone temperature T_v. The vapor zone contains oil and water in both liquid and gaseous forms. In the presence of oxygen (that may partially pass through the combustion zone), slow oxidation occurs in the vapor zone at lower temperatures. When the gas reaches the original cold reservoir, part of the oil vapor and water condenses. This solution structure is called reaction-leading because combustion occurs ahead of the hot zone.

In this paper, we are only interested in the part of the whole structure upstream of the vapor zone. In the vapor zone, the concentrations n_h^*, n_c^*, n_v^* as well as the temperature T_v are determined by the condensation and flow processes far downstream (right) of the reaction wave, which represent a separate problem. In our study of combustion, we assume these quantities to be known. The unknown parameters of the reaction wave to be determined are the temperature T_h, the reaction wave speed υ, the gas flux change in the wave and the amount of oxygen that passes through unburned.

The oil vapor and steam released in the reaction wave due to cracking and vaporization increase the molar gas flux by $\upsilon n_c^* / M_c$ and $\upsilon n_v^* / M_v$. In the vapor zone the gas flux is given by

$$\left(\rho u\right)_v = \left(\rho u\right)_{inj} + \upsilon\left(n_c^* / M_c + n_v^* / M_v\right). \tag{10}$$

The formulae below are given for the typical case of in-situ combustion, when the contribution of cracking and vaporization in the total heat balance and molar gas flux in the reaction wave are small. More general formulae that do not use this assumption can be found in the Appendix "*Reaction leading structure*".

There are two different combustion regimes with reaction-leading structure. They correspond to complete consumption of coke and either complete or partial consumption of oxygen in the HTO reaction. In the regime of complete oxygen consumption, the wave speed and highest temperature in the wave given below are based on mass and heat balance considerations (see Appendix "*Reaction leading structure*" and Mailybaev et al. 2010)

$$\upsilon = \frac{\left(\rho u Y\right)_{inj} M_h}{n_h^*}, \quad T_h = T_v + \frac{\upsilon Q_h n_h^*}{\upsilon C_m - c_g \left(\rho u\right)_{inj}}. \tag{11}$$

The first equation expresses that υ is the fuel consumption rate and the second equation expresses that the combustion heat is used to heat up the space between the thermal wave traveling at a speed υ_T and the combustion front traveling at speed υ. Complete oxygen consumption only occurs if the reaction zone is sufficiently long, the temperature and reaction rate are sufficiently high, i.e.,

$$\frac{\lambda R T_h^2 K_h n_h^*}{E_h Q_h Y_{inj} \left(\rho u\right)_{inj}^2 M_h^2} \exp\left(-\frac{E_h}{R T_h}\right) > 1. \tag{12}$$

Eq. (12) introduces Zeldovich's concept described in Appendix "*High temperature oxidation region"*.

If condition (12) is not satisfied, a considerable part of oxygen is not consumed in the reaction. This is the situation we address now. We can use the second equation (11) also for incomplete oxygen consumption written as

$$\upsilon = \frac{c_g \left(\rho u\right)_{inj}}{C_m - Q_h n_h^* / \left(T_h - T_v\right)}. \tag{13}$$

The Zeldovich approach gives us an implicit expression for T_h in case of incomplete oxygen consumption, i.e.,

$$\frac{\lambda R T_h^2 K_h Y_{inj}}{E_h Q_h n_h^* \upsilon^2} \exp\left(-\frac{E_h}{RT_h}\right) = 1, \tag{14}$$

where υ must be substituted from (13). This implicit equation can be solved using a numerical program for a single non-linear equation. The lower bound for T_h to be used in the program is

$$T_h > T_v + \frac{Q_h n_h^*}{C_m - c_g n_h^* / \left(Y_{inj} M_h\right)}. \tag{15}$$

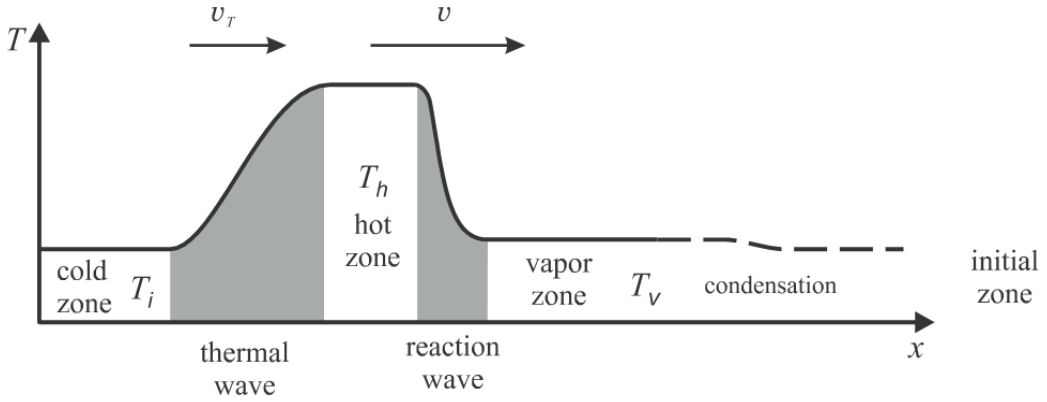

Figure 1: Reaction-leading structure. The reaction wave is faster than the thermal wave. The cold and hot zones contain air. The vapor zone contains oil, water, and gas with oil vapor, steam and combustion products.

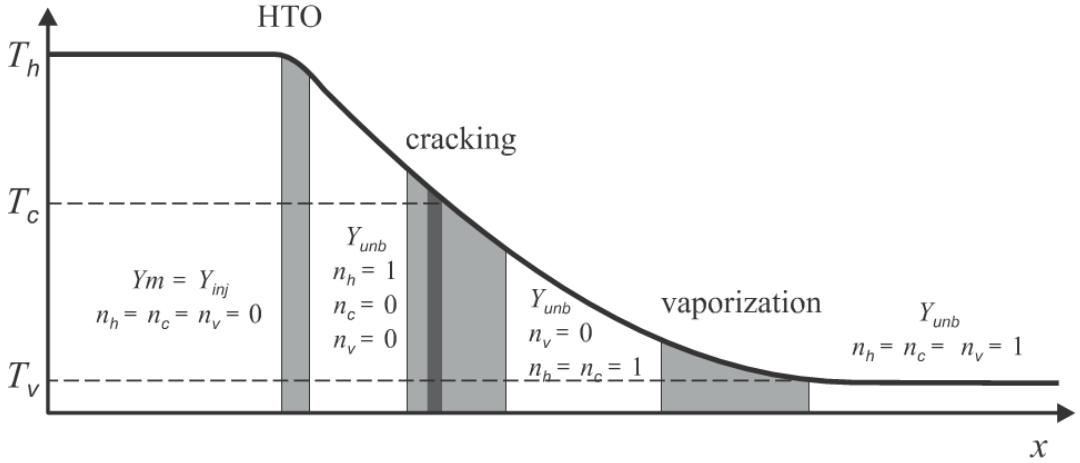

Figure 2: Reaction wave internal structure: HTO, cracking and vaporization regions. Cracking of each component occurs in a thin region within the cracking zone. The values of oxygen flux Ym and oil components concentrations n_h, n_c, n_v are specified in each region.

Equating the consumption of oxygen to the consumption of coke we obtain

$$\left(\rho u Y\right)_{inj} - \left(\rho u Y\right)_{unb} = \upsilon n_h^* / M_h. \tag{16}$$

In this way we can calculate the mole fraction of unburned oxygen Y_{unb}. Requiring that Y_{unb} in (16) is nonnegative together with the condition $\upsilon_T < \upsilon$ and υ_T from (9), we can show that

$$\left(\rho u Y\right)_{inj} > \upsilon_T \frac{n_h^*}{M_h} = \frac{\left(\rho u\right)_{inj} c_g}{C_m} \frac{n_h^*}{M_h} \quad \text{or} \quad Y_{inj} > \frac{c_g n_h^*}{C_m M_h}. \tag{17}$$

This condition is satisfied in most practical situations, unless the injected gas contains very little oxygen.

Applying the concept of Zeldovich in the cracking zone shows that the temperature T_c satisfies the equation

$$\frac{RT_c^2 K_c}{2\upsilon E_c \left|T_c'\right|}\exp\left(-\frac{E_c}{RT_c}\right)=1, \tag{18}$$

where

$$T_c' = -Q_h n_h^* \upsilon/\lambda + C_m\left(\upsilon-\upsilon_T\right)\left(T_h-T_c\right)/\lambda. \tag{19}$$

Using (19), equation (18) can be solved numerically, furnishing the cracking temperature T_c. This is an average cracking temperature, when K_c and E_c are effective cracking kinetic coefficients. In a more realistic model, each medium oil component cracks in a thin region near the corresponding temperature T_c, see Fig. 2 (thin dark interval within a wider cracking zone). This temperature is determined by the same equations (18), (19), where K_c and E_c are the kinetic coefficients corresponding to this specific component. The position of the cracking region in the wave can also be computed for each component, as shown in Appendix "*Reaction leading structure*".

Of course, for our solution to be correct, it is important that $T_c < T_h$ for each medium oil component. Otherwise, medium oil remains in the HTO zone and participates in the HTO reaction.

Reaction trailing structure

The reaction-trailing structure is shown in **Fig. 3**. The coke oxidation reaction occurs in a slow HTO wave traveling with speed υ. The temperature in this wave changes from a high value T_h in the hot zone ahead of the wave to the injected air temperature T_i behind. The cracking reaction and oil vaporization take place in another wave traveling with higher speed $\upsilon_T > \upsilon$. If there were neither medium oil nor light oil/water in the reservoir, this wave would be just a thermal wave with speed (9). The hot region between the two waves contains coke with concentration n_h^* but neither medium oil nor light oil/water. As in the previous section we assume that the oil component concentrations $n_h^*,\ n_c^*,\ n_v^*$ and the temperature T_v in the vapor zone ahead of the thermal wave region are given.

Since the hot region ahead of the HTO wave contains coke, oxygen is consumed completely in the HTO reaction. Coke consumption is not necessarily complete, so the HTO reaction is oxygen controlled. This solution structure is called reaction-trailing because combustion occurs behind the hot zone. The existence of the hot zone between the HTO and thermal wave ensures that complete cracking of the medium oil occurs ahead of the HTO wave.

The only reaction in the HTO wave is coke oxidation. There are two different combustion regimes in the reaction-trailing structure, corresponding to either complete or partial consumption of coke in the HTO reaction. The derivation is similar as for the reaction leading structure and therefore we do not go into details, see the Appendix "*Reaction trailing structure*". In the regime of complete coke consumption, the wave speed and the highest temperature in the HTO wave are

$$\upsilon = \frac{\left(\rho u Y\right)_{inj} M_h}{n_h^*}, \quad T_h = T_i + \frac{\upsilon Q_h n_h^*}{c_g\left(\rho u\right)_{inj} - \upsilon C_m}. \tag{20}$$

This regime is determined by condition (12).

If (12) is not satisfied, the unburned concentration of coke is given by n_h^{unb}. In this case, the wave speed is related to the combustion temperature T_h by

$$\upsilon = \upsilon_T - \frac{Q_h\left(\rho u Y\right)_{inj} M_h}{C_m\left(T_h - T_i\right)}. \tag{21}$$

The temperature T_h is determined implicitly by the equation

$$\frac{\lambda RT_h^2 K_h n_h^*}{E_h Q_h\left(\rho u\right)_{inj}^2 Y_{inj} M_h^2}\exp\left(-\frac{E_h}{RT_h}\right)=1. \tag{22}$$

This equation is solved using a numerical solver for a single algebraic equation, with lower bound

$$T_h > T_i + \frac{Q_h n_h^*}{c_g n_h^* / \left(Y_{inj} M_h\right) - C_m}. \tag{23}$$

The unburned coke concentration left behind the HTO wave is

$$n_h^{unb} = n_h^* - \left(\rho u Y\right)_{inj} M_h / \upsilon. \tag{24}$$

The thermal wave speed is approximately equal to (9). However, cracking and vaporization that occur in this wave slightly decrease the value in (9) as shown in Appendix "*Reaction trailing structure*". The gas flux in the vapor zone is given similarly to (10) as

$$\left(\rho u\right)_v = \left(\rho u\right)_{inj} + \upsilon_T \left(n_c^* / M_c + n_v^* / M_v\right). \tag{25}$$

Requiring that (24) is nonnegative and using the condition $\upsilon_T > \upsilon$ with υ_T from (9), we obtain

$$Y_{inj} < \frac{c_g n_h^*}{C_m M_h}. \tag{26}$$

This is opposite to (17). It is satisfied when the coke concentration is large or the oxygen concentration in the injected air is small.

We conclude that the reaction-leading combustion wave occurs under condition (17). Otherwise, we have the reaction-trailing structure. The regime with complete consumption of coke and oxygen in the HTO is determined by (12), where T_h is given by (11) for the reaction-leading structure and by (20) for the reaction-trailing structure. If (12) is not satisfied, a considerable part of oxygen or coke is not consumed, respectively, in the reaction-leading and reaction-trailing cases.

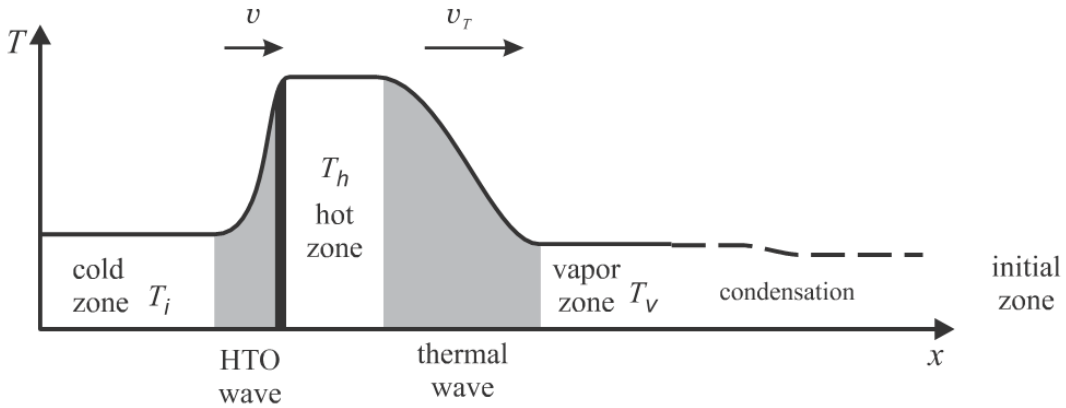

Figure 3: Reaction-trailing structure. The HTO wave is slower than the thermal wave; a thin region where the HTO reaction occurs is shown black. The cold zone contains air. The hot zone contains coke and gas with combustion products. The vapor zone contains oil, steam, and gas with oil vapor, steam and combustion products.

In-situ combustion for typical reservoir parameters

Consider the typical reservoir data in Table 1. The numbers quoted correspond to octene ($C_8 H_{16}$) as an effective light oil component, hexadecene ($C_{16} H_{32}$) as a medium oil component, and average vaporization heat Q_v for a liquid mixture with equal light oil and water concentrations in the vapor zone. .

Assume that air with oxygen fraction Y_{inj} = 0.21 is injected into the reservoir. Condition (9) is satisfied for precoke concentrations n_h^* < *173* [kg/m^3] in the vapor zone. This is the case of the reaction-leading wave structure. **Fig. 4** shows the reaction wave parameters versus the initial precoke concentration n_h^* [kg/m^3], when the other parameters in the vapor zone are taken as n_c^* =*100* [kg/m^3] and n_v^* = *60* [kg/m^3] and T_v =77 °C. Complete coke and oxygen consumption in the HTO reaction occurs for high precoke concentrations n_h^* > *35.5* [kg/m^3], as found by checking inequality (12). For lower precoke concentrations, a considerable part of the injected oxygen passes through the reaction zone, as shown in Fig. 4. The transition from complete to partial oxygen consumption regime is characterized by an abrupt change in the dependence of the variables relative to the coke concentration n_h^*.

Parameter	Meaning	Value
Q_h	HTO reaction enthalpy	3.28×10^7 J/kg
Q_c	cracking reaction enthalpy	3.39×10^5 J/kg
Q_v	vaporization heat	1.28×10^6 J/kg
E_h	activation energy (HTO)	1.8×10^5 J/mol (Smith 1978)
K_h	Pre-exponential factor (HTO)	3.05×10^6 1/s (Smith 1978)
E_c	activation energy (cracking)	2.5×10^5 J/mol
K_c	Pre-exponential factor (cracking)	4.6×10^{14} 1/s
R	Gas constant	8.314 J/mol K
C_m	heat capacity of rock	2×10^6 J/m^3 K
λ	thermal conductivity of rock	0.87 W/mK
c_g	heat capacity of gas	3.5*R* J/mol K
P_{tot}	prevailing pressure of gas	10^5 Pa (1 atm)
u_{inj}	Darcy velocity of injected gas	1.16×10^{-3} m/s (100 m/day)
M_h	molar weight of carbon	0.012 kg/mol
M_c	average molar weight of cracked oil	0.112 kg/mol
M_v	average molar weight of liquid oil and water	0.065 kg/mol
$T_i = T_{st}$	injected gas temperature	293.15 K

Table 1: Typical values of dimensional parameters for in-situ combustion.

Fig. 4 at the right shows the velocities of the combustion wave (υ), thermal wave (υ_T), together with the curve for Y_{inj}. For low values of n_h^* we observe that there is a point where the speeds coincide $\upsilon_T = \upsilon$, however for a large value of $Y_{unb} \sim Y_{inj}$, meaning that there is essentially no combustion. Also for the large value $n_h^* = 173$ [kg/m^3] (outside Fig. 4 to the right), there is another point with coinciding speeds. It is the resonance point with complete oxygen consumption $Y_{unb} = 0$ lying on the resonance line in **Fig. 6.**

Calculations verify that changes in medium and light oil/water concentrations have very minor influence on the combustion and cracking temperatures T_h and T_c. Indeed, the corresponding equations (14) and (18) have strong exponential dependence on temperature, so the solutions are weakly affected by a change of coefficients. The speed υ of the reaction wave decreases slightly with increase of medium and light oil/water concentrations.

Consider now the same reservoir parameters in the vapor zone, but an injected gas with very low initial oxygen fraction Y_{inj} = 0.025. The numerical results are shown in **Fig. 5**. Condition (17) is satisfied for precoke concentrations $n_h^* < 20.6$ [kg/m^3] and corresponds to the reaction-leading structure studied in the corresponding section. Higher concentrations lead to the reaction-trailing wave structure and calculations use the formulae of the corresponding section These two cases are separated by a resonance point, where the speeds of the two waves coincide: $\upsilon = \upsilon_T$. The complete coke/oxygen consumption regime is determined by the inequality (12) and corresponds to 14.5 < n_h^* < 44.9 [kg/m^3]. Temperatures in this region become very high. On the contrary, the partial oxygen (n_h^* < 14.5 [kg/m^3]) and partial coke (n_h^* > 44.9 kg/m^3) consumption regimes are characterized by almost constant combustion temperature. The dependence of the HTO wave parameters on n_h^* possesses a singularity when the regime changes.

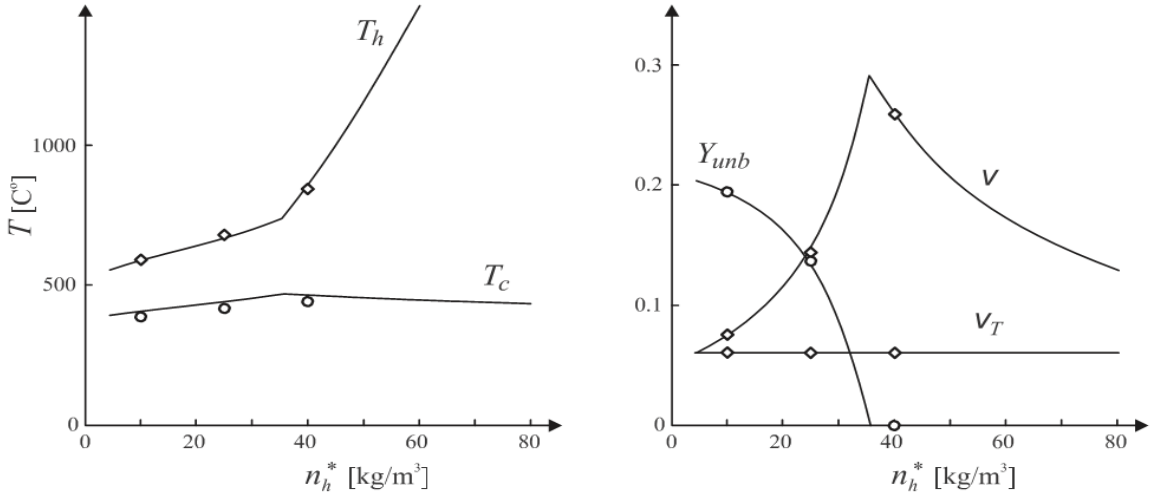

Figure 4: Reaction wave parameters depending on precoke concentration n_h^* [kg/m^3] with n_c^* = 100 [kg/m^3], and n_v^*=60 [kg/m^3] for injection of air with 21% of oxygen. The vapor zone temperature is T_v = 77 [^{o}C]. The hot zone temperature is T_h [^{o}C], the cracking temperature is T_c [^{o}C], the HTO and thermal wave speeds are denoted by v, v_T [m/day], the unburned oxygen fraction is Y_{unb}. Results of numerical simulations are presented for n_h^* = 10, 25, 40 [kg/m^3].

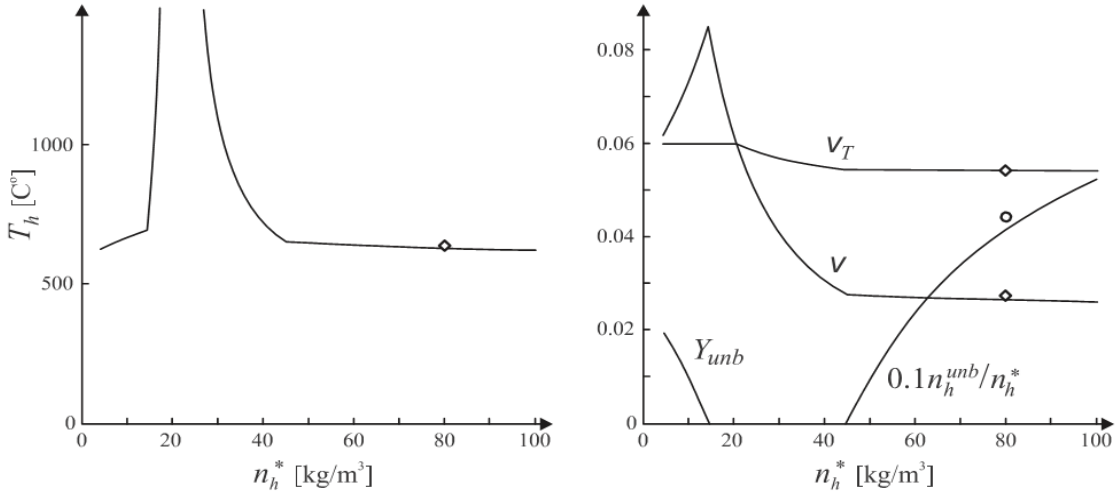

Figure 5: HTO and thermal waves parameters depending on precoke concentration n_h^* [kg/m^3] with n_c^* = 100 [kg/m^3], and n_v^*=60 [kg/m^3] for injection of air with reduced oxygen (2.5%). The hot zone temperature is T_h [^{o}C], the HTO and thermal wave speeds are denoted by v, v_T [m/day], the unburned oxygen fraction is Y_{unb}, the unburned coke fraction n_h^{unb}/n_h^*. Results of numerical simulations are presented for n_h^* = 80 [kg/m^3].

Fig. 6 presents a chart with different combustion regimes in the $\left(n_h^*, Y_{inj}\right)$ plane: coke concentration versus oxygen fraction in the injected air. The boundary between the reaction-leading and reaction-trailing combustion structures is determined by the straight resonance line $Y_{inj} = n_h^* c_g / \left(C_m M_h\right)$, see (17), (26). The boundary of the regime with complete consumption of coke and oxygen, shown white in Fig. 6, is determined by (12) written as equality. Here we must substitute T_h from (11) to determine the boundary with the domain corresponding to partial oxygen consumption, or T_h from (20) to determine the boundary with the domain corresponding to partial coke consumption. There is also a boundary corresponding to extinction at small coke concentration n_h^*. This branch of points, characterized by low oxygen consumption, is still under

investigation and is therefore not yet included in Fig. 6. We conjecture that such extinction occurs in situations where the combustion heat $Q_h n_h^*$ attains certain values close to the heat $Q_c n_c^* + Q_v n_v^*$ necessary for cracking and vaporization and the speeds of the two waves coincide, $\upsilon_T = \upsilon$, see Eqs. (38) and (41). The speed υ gets close to υ_T also for very small injected oxygen fractions Y_{inj}, as one can show using Eqs. (21), and (22). The chart of combustion regimes has the qualitative form shown in Fig. 6 for a wide range of parameters.

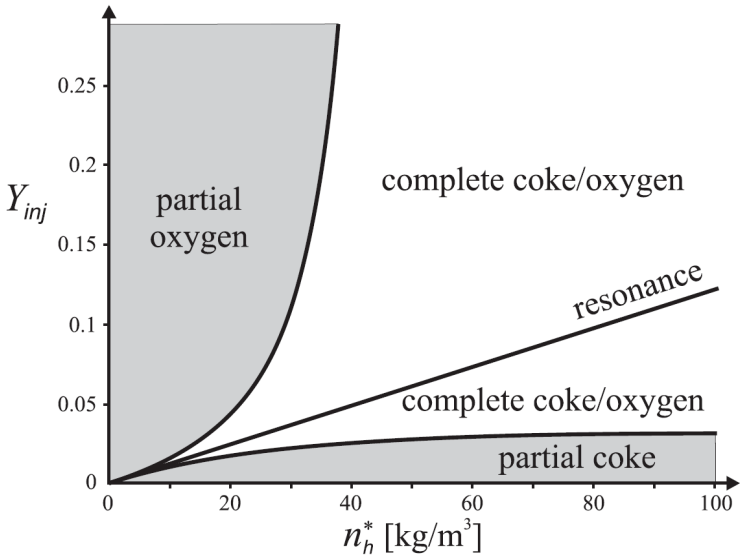

Figure 6: Chart of combustion regimes for different coke concentrations n_h^* [kg/m^3] and injected oxygen fractions Y_{inj}. Resonant states form a straight line that separates combustion regimes with different wave structures: reaction-leading (above the line) and reaction-trailing (below the line). The gray regions correspond to combustion regimes with partial oxygen and partial coke consumption. The white region corresponds to the complete coke and oxygen consumption.

Numerical simulation

We performed direct numerical simulation of the PDE system (2)-(8) using a split-implicit finite difference scheme. In order to define the vaporization rate W_v, we introduce the mole fraction X of light oil vapor and steam in gas. The change of total gas flux ρu in the model is due to cracked and vaporized components and it equals $\rho u X$. Therefore, we find further downstream $\rho u = (\rho u)_{inj} + \rho u X$ and $X = 1 - (\rho u)_{inj} / \rho u$. As we already mentioned above, the details of the vaporization process have a minor influence on the reaction waves of interest here. So, for numerical purposes we can use a simplified model, which reflects only qualitative properties of vaporization: $W_n = k n_v (X_{eq} - X)$ with $k = 10^{-4}\ s^{-1}$, $X_{eq} = \exp((T - T_b)/h)$, $h = 25\ K$ and T_b determined by the equilibrium condition in the vapor zone.

The reaction-leading and reaction-trailing wave structures were observed in numerical simulation with initial temperatures high enough for ignition to occur in a reasonable time span and for different oil concentrations in the initial reservoir and oxygen fractions in the injected gas. The dimensional parameters of the reaction and thermal waves obtained in this simulation are shown in Figs. 4 and 5; we see very good agreement between theoretical and numerical results.

The reaction (HTO) waves were found to be stable traveling waves in numerical simulation, except for the case of n_h^* = *25* [kg/m^3] in Fig. 4. In the latter case the reaction wave speed υ oscillates periodically in time; Fig. 4 shows the average values of corresponding quantities. Oscillation amplitudes are about 7% of the average value for T_h and about 30% for υ and Y_{unb}. Therefore, some part of the chart in Fig. 6 corresponds to oscillating solutions. Using results of stability analysis of combustion waves obtained in Aldushin and Kasparyan 1981, one can derive stability conditions for steady traveling reaction wave and identify the region of pulsating regimes, see Mailybaev et al. 2010.

Conclusion

We derived analytical formulae for in-situ forward combustion by air injection in porous media, containing crude oil and water. The oil components are grouped into precoke, medium and light oil pseudo-components. These pseudo-components participate in different chemical and physical processes. Precoke is converted to coke at high temperatures, medium oil components are cracked at slightly lower temperatures releasing gaseous oil, while light oil components and water are vaporized. Heat is released mainly in the high-temperature oxidation of coke.

The solutions are found in the form of sequences of waves. It turns out that it is possible to distinguish between two combustion regimes according to the relative position of the hot zone and high-temperature oxidation region: reaction-leading and reaction-trailing wave structures. At low precoke concentrations or high injected oxygen fractions, the HTO region lies downstream of the hot zone. At high precoke concentrations or low injected oxygen fractions, the HTO region lies upstream of the hot zone.

Each structure occurs in two different combustion regimes. In the first regime, both coke and oxygen are completely consumed in the combustion. In the second regime, only a part of oxygen is consumed for the reaction-leading wave structure, or a part of coke is consumed for the reaction-trailing wave structure. The typical chart with four combustion regimes is shown in Fig. 6.

We derived explicit analytical conditions for each combustion regime as well as formulae describing dependent variables in the wave sequence solutions. Additionally we described the internal structure of the oil cracking zone for the reaction-leading wave structure. We developed a simplified method for analysis of the combustion region. In this method, rather than explicitly integrating wave equations, we use general estimates and exploit strong exponential dependence of combustion rate on temperature to simplify the results. This procedure is general and can be applied to the analysis of reaction zones characterized by large Zeldovich numbers, as we did in the paper both for the high-temperature oxidation and cracking regions.

Numerical computations with typical reservoir data for in-situ combustion lead to the following observations. The most typical wave structure is reaction-leading. With increasing coke concentration, the partial oxygen consumption regime changes into the complete coke/oxygen consumption regime. The first regime is characterized by weak dependence of combustion temperature to reservoir parameters, while the temperatures may become very high in the complete coke/oxygen consumption regime. The reaction-trailing structure can also be found when the injected air contains reduced amounts of oxygen (for example, for injection of a mixture of air and flue gas). Numerical simulation of the full system of governing equations was carried out showing expected accuracy of our asymptotic formulae. For some reservoir parameters, the steady reaction wave turned out to be unstable, and combustion occurred in a wave traveling with a speed changing periodically in time.

The work described has the following practical applications: (1) validation of numerical simulation programs, (2) accurate risk assessment of oxygen breakthrough by anayzing the detailed structure of the reaction zone avoiding numerical artifacts, (3) quick evaluations of consequences of different injection conditions given the kinetic behavior of the oil under consideration.

References

J. H. Abou-Kassem, S. M. Farouq Ali, and J. Ferrer. Appraisal of steamflood models. *Rev. Tec. Ing.*, 9:45-58, 1986.

S.A. Abu-Khamsin, W.E. Brigham, and H.J. Ramey. Reaction kinetics of fuel formation for in-situ combustion. *SPE Reserv. Eng*, Vol **3** (4) 1988.

S. Akin, M. V. Kok, S. Bagci, and O. Karacan. Oxidation of heavy oil and their SARA fractions: Its role in modeling in-situ combustion. SPE 63230, 2000.

I. Y. Akkutlu and Y. C. Yortsos. The dynamics of in-situ combustion fronts in porous media. *Combustion and Flame*, 134:229-247, 2003.

A. P. Aldushin, A. Bayliss, and B. J. Matkowsky. On the transition from smoldering to flaming. *Combustion and Flame*, 145:579-606, 2006.

A. P. Aldushin and S. G. Kasparyan. Stability of stationary filtrational combustion waves. *Combustion, Explosion, and Shock Waves*, 17(6):615-625, 1981.

A. P. Aldushin, B. J. Matkowsky, and D. A. Schult. Downward buoyant filtration combustion. *Combustion and Flame*, 107:151-175, 1996.

A. P. Aldushin, B. J. Matkowsky, and D. A. Schult. Buoyancy driven filtration combustion. *Combustion Science and Technology*, 125:283-349, 1997.

A. Bayliss and B. J. Matkowsky. From traveling waves to chaos in combustion. *SIAM J. Appl. Math.*, 54:147-174, 1994.

P. C. Bowes and P. H. Thomas. Ignition and extinction phenomena accompanying oxygendependent self-heating of porous bodies. *Combustion and Flame*, 10:221-230, 1966.

J. Bruining, A. A. Mailybaev, and D. Marchesin. Filtration combustion in a wet porous medium. *SIAM J. Appl. Math.*, 70:1157-1177, 2009.

H. Byrne and J. Norbury. The effect of solid conversion on travelling combustion waves in porous media. *Journal of Engineering Mathematics*, 32:321-342, 1997.
L. M. Castanier and W. E. Brigham. Modifying in-situ combustion with metallic additives. *In Situ*, 21:27-45, 1997.
L. M. Castanier and W. E. Brigham. Upgrading of crude oil via in situ combustion. *Journal of Petroleum Science and Engineering*, 39:125-136, 2003.
D. N. Dietz and J. Weijdema. Wet and partially quenched combustion. *Journal of Petroleum Technology*, 20:411-415, 1968.
M. G. Gerritsen and L. J. Durlofsky. Modeling fluid flow in oil reservoirs. *Annual Review of Fluid Mechanics*, 37:211-238, 2005.
M. V. Kok and C. 0. Karacan. Behavior and effect of SARA fractions of oil during combustion. *SPE Reservoir Evaluation and Engineering*, 3:380-385, 2000.
M. R. Kristensen, M. G. Gerritsen, P. G. Thomsen, M. L. Michelsen, and E. H. Stenby. Efficient integration of stiff kinetics with phase change detection for reactive reservoir processes. *Transport in Porous Media*, 69:383-409, 2007.
C. S. Kuhn and R. L. Koch. In-Situ Combustion: Newest Method of Increasing Oil Recovery. *Oil and Gas Journal*, 52(14):92, 1953.
C. Y. Lin, W. H. Chen, and W. E. Culham. New kinetic models for thermal cracking of crude oils in in-situ combustion processes. *SPE Reservoir Engineering*, 2:54-66, 1987.
C. Y. Lin, W. H Chen, S. T. Lee, and W. E. Culham. Numerical simulation of combustion tube experiments and the associated kinetics of in-situ combustion processes. *SPE Journal*, 24:657-666, 1984.
A. A. Mailybaev, J. Bruining, and D. Marchesin. Analysis of in-situ combustion regimes with pyrolysis and vaporization. *Combustion and Flame (submitted)*, 2010.
B. J. Matkowsky and G. Sivashinsky. Propagation of a pulsating reaction front in solid fuel combustion. *SIAM J. Appl. Math.*, 35:465-478, 1978.
H. J. Ramey Jr. Discussion on development of an underground heat wave for oil recovery. *J. Pet. Tech.*, pages 32-33, 1954.
D. A. Schult, A. Bayliss, and B. J. Matkowsky. Traveling waves in natural counterflow filtration combustion and their stability. *SIAM J. Appl. Math.*, 58:806-852, 1998.
D. A. Schult, B. J. Matkowsky, V. A. Volpert, and A. C. Fernandez-Pello. Forced forward smolder combustion. *Combustion and Flame*, 104:1-26, 1996.
I. W. Smith. The intrinsic reactivity of carbons to oxygen. *Fuel*, 57:409-414, 1978.
C. W. Wahle, B. J. Matkowsky, and A. P. Aldushin. Effects of gas-solid nonequilibrium in filtration combustion. *Combust. Sci. and Tech.*, 175:1389-1499, 2003.
J. Weijdema. Zur oxydationskinetik kohlenwasserstoffe in porTosen medien in bezug auf untererdische verbrennung. *Erdol und Kohle, Erdgas Petrochemie*, 21:520-526, 1968.
Y. B. Zeldovich, G. I. Barenblatt, V. B. Librovich, and G. M. Makhviladze. *The mathematical theory of combustion and explosion*. Consultants Bureau, New York, 1985.

Appendices

High-temperature oxidation region

The region where HTO takes place in a combustion wave contains coke and injected gas with oxygen, combustion products and some inert gas. The highest temperature in the reservoir T_h is reached in this region. As all medium and light oil components are cracked and vaporized downstream, the molar gas flux in the HTO region is the injected gas flux $(\rho u)_{inj}$. It remains constant because one mole of O_2 is converted to one mole of CO_2. The injected oxygen molar flux is $(\rho u Y)_{inj}$. The coke concentration ahead of the HTO region is n_h^*.

The reaction rate (7) has strong temperature dependence determined by the exponent. Therefore we can only afford a very small temperature variation δT_h in the reaction zone. Expanding the exponent near T_h, for small $\delta T_h = T_h - T$ we find

$$\exp\left(-\frac{E_h}{RT}\right) \approx \exp\left(-\frac{E_h}{RT_h}\right)\exp\left(-\frac{Z_h \delta T_h}{(T_h - T_v)}\right) \tag{27}$$

with

$$Z_h = \frac{E_h (T_h - T_v)}{RT_h^2}, \tag{28}$$

where $Z_h >> 1$ because the activation energy E_h is large (a typical value is $Z_h \sim 15$). The last exponential in expression

(27) is a reduction factor in the reaction rate, and the reaction ceases when this factor becomes small. Thus, the reaction occurs within a small temperature interval $\delta T_h \sim \left(T_h - T_v\right)/Z_h$ that corresponds to a change of order 1 in the exponent; the reaction rate decreases rapidly and becomes negligibly small for lower $T < T_h - \delta T_h$. The dimensionless quantity Z_h is the Zeldovich number, the ratio between the total temperature variation in the wave and the temperature variation in the HTO region (Zeldovich et al. 1985). Using the expression for δT_h, we find that the HTO reaction is confined within the space interval

$$\delta x_h \sim \frac{\delta T_h}{\left|T_h'\right|} \sim \frac{T_h - T_v}{Z_h \left|T_h'\right|}, \tag{29}$$

where $\left|T_h'\right|$ is the effective temperature gradient in the HTO region (the prime denotes the derivative $\partial/\partial x$). For $Z_h \sim 1$, δx_h is much smaller than the width of the whole wave, which is estimated as $\left(T_h - T_v\right)/\left|T_h'\right| \sim Z_h \delta x_h$, so the HTO region is thin.

The maximal concentrations of coke and oxygen in the HTO region equal n_h^* and Y_{inj}, and at least one of them is completely consumed in the reaction. Thus, using the estimate $Yn_f \sim Y_{inj} n_f^*/2$ and $T \approx T_h$ in (7), we find the effective HTO rate in the combustion zone

$$W_h^* \sim K_h \left(Y_{inj} n_h^*/2\right) \exp\left(-\frac{E_h}{RT_h}\right). \tag{30}$$

Complete consumption of coke and oxygen

In this case, $\upsilon n_h^*/M_h$ moles of coke burn per unit time and per unit wave surface area, where υ is the combustion wave speed. For the reaction $C+O_2 \rightarrow CO_2$, it is equal to the molar oxygen flux $\left(\rho u Y\right)_{inj}$ in the injected air. This determines the combustion propagation speed in (11).

The temperature gradient vanishes on one side of the HTO region. On the other side it can be determined by comparing the heat $Q_h n_h^* \upsilon$ generated per unit time with the heat flux $\lambda T'$ due to heat conductivity. This comparison yields $T' = -Q_h n_h^* \upsilon/\lambda$. The average gradient in the HTO region is, therefore,

$$\left|T_h'\right| \sim \frac{1}{2\lambda} Q_h n_h^* \upsilon = \frac{1}{2\lambda} Q_h \left(\rho u Y\right)_{inj} M_h \tag{31}$$

Using (28), (31) in (29), we find the width of the reaction zone

$$\delta x_h \sim \frac{2\lambda R T_h^2}{E_h Q_h \left(\rho u Y\right)_{inj} M_h}, \tag{32}$$

which is determined by the temperature dependence of the reaction rate.

We sketch the derivation for Eq. (12) as follows. As the amount of oxygen equals the amount of carbon consumed, we can use Eq. (7) to show that

$$-\frac{\partial \ln Y}{\partial x} = \frac{W_h}{\rho u Y M_h} \sim \frac{K_h n_h^*}{2\left(\rho u\right)_{inj} M_h} \left(-\frac{E_h}{RT_h}\right). \tag{33}$$

Integration over the interval δx_h essential for the HTO reaction leads to

$$\ln\left(\frac{Y_{inj}}{Y_{unb}}\right) \sim \frac{K_h n_h^*}{2\left(\rho u\right)_{inj} M_h} \exp\left(-\frac{E_h}{RT_h}\right) \delta x_h. \tag{34}$$

When the right side of (35) exceeds one, almost complete oxygen consumption occurs. Substitution of (32) leads to the complete oxygen consumption condition (12).

Partial oxygen consumption

Oxygen may not be consumed in the reaction zone completely so that a considerable mole fraction Y_{unb} of oxygen remains in the gas downstream of the HTO region. The flux of consumed oxygen $\left(Y_{inj}-Y_{unb}\right)\left(\rho u\right)_{inj}$ reacts with an equal molar amount of coke $\upsilon n_h^*/M_h$. This yields (16).

The average temperature gradient in the HTO region

$$|T_h'|\sim Q_h n_h^*\upsilon/\left(2\lambda\right) \tag{35}$$

as is found as in (31), except that υ is unknown. Then (28), (29) give

$$\delta x_h \sim \frac{2\lambda R T_h^2}{E_h Q_h n_h^* \upsilon}. \tag{36}$$

In this case both coke and oxygen are present on one side of the HTO region, where the reaction stops due to low temperature. Thus, the reaction occurs within the whole interval δx_h and the total reaction rate is estimated as $W_h^*\delta x_h$. Equating this rate to the amount of coke $n_h^*\upsilon$ burned per unit time, we obtain (14). Here we used (30), (36) and replaced the ~ sign by an equality with relative accuracy of order Z_h^{-1} for T_h, as we did in (12).

Partial coke consumption

Oxygen is consumed completely, but part of coke with concentration n_h^{unb} remains in the burned region behind the combustion wave. The combustion wave speed is determined by equating the burned coke rate $(n_h^*-n_h^{unb})\upsilon/M_h$ with oxygen flux $\left(\rho uY\right)_{inj}$, obtaining

$$\upsilon=\left(\rho uY\right)_{inj}M_h/(n_h^*-n_h^{unb}). \tag{37}$$

Following the same derivations as in the case of partial oxygen consumption above, but with the burned coke concentration taken as $n_h^*-n_h^{unb}=\left(\rho uY\right)_{inj}M_h/\upsilon$, we obtain (22) instead of (14).

Reaction-leading structure

The total heat released in the reaction wave per unit time equals υQ, where

$$Q=Q_h n_h^*-Q_c n_c^*-Q_v n_v^*. \tag{38}$$

The heat rate $c_g\left(\rho u\right)_{inj}(T_h-T_{st})-c_g\left(\rho u\right)_v(T_v-T_{st})$ transported by the gas together with (38) contribute to the heat accumulated in the hot zone behind the reaction wave and equally

$$\upsilon Q+c_g\left(\rho u\right)_{inj}(T_h-T_{st})-c_g\left(\rho u\right)_v(T_v-T_{st})=\upsilon C_m\left(T_h-T_v\right). \tag{39}$$

Using (9), (10), equation (39) is solved for T_h as

$$T_h=T_v+\frac{\upsilon Q}{C_m\left(\upsilon-\upsilon_T\right)}, \tag{40}$$

where we neglected the small term $-(T_v-T_{st})c_g\upsilon\left(n_c^*/M_c+n_v^*/M_v\right)$ in the denominator. When solved for υ, Eq. (40) leads to

$$\upsilon=\frac{\upsilon_T}{1-Q/(C_m(T_h-T_v))}. \tag{41}$$

For $Y_{unb}>0$, (16) gives $\upsilon<\left(\rho uY\right)_{inj}M_h/n_h^*$. Substituting $\upsilon=\left(\rho uY\right)_{inj}M_h/n_h^*$ into (40) yields a lower bound for T_h. The terms containing n_c^* and n_v^* in Q are usually small and can be neglected. This simplification is used in (11), (13), (15).

Cracking region

Due to its high activation energy, the cracking reaction occurs in a thin region near the corresponding temperature T_c. The cracking region is thin due to the cracking rate given in (8) for the data in Table 1. The analysis of the cracking region will be presented in short form, because it has much in common with the analysis of the HTO region.

The reaction is mostly confined within a small temperature interval $\delta T_c \sim \left(T_c - T_v\right)/Z_c$ with a large Zeldovich number $Z_c = E_c\left(T_c - T_v\right)/\left(RT_c^2\right) >> 1$. As in (29), the width of the cracking region is $\delta x_c = \left(T_c - T_v\right)/\left(Z_c\left|T_c'\right|\right)$, where $\left|T_c'\right|$ is the effective temperature gradient in the region. The expression for the effective cracking rate in the region is similar to (30), i.e., $W_c^* \sim K_c\left(n_c^*/2\right)\exp\left(-E_c/\left(RT_c\right)\right)$. The cracking temperature can be found from the medium oil balance relation $W_c^*\delta x_c \sim \upsilon n_c^*$ as (18), where the ~ sign is replaced by equality, which is a good approximation for large Z_c, see Appendix "*High temperature oxidation region*".

The heat and gas production in the cracking zone is always small. Then in the region between the HTO and cracking regions $(\rho u) \approx (\rho u)_{inj}$. The heat equation (6) takes the form

$$-\upsilon C_m T' + c_g\left(\rho u\right)_{inj} T' = \lambda T'', \tag{42}$$

where $\partial/\partial t = -\upsilon\partial/\partial x$ in a traveling wave moving with speed υ. Setting $x = 0$ at the HTO region, we have $T(0)=T_h$. As we showed in the Appendix "*Complete consumption of coke and oxygen*", the temperature gradient ahead of the HTO region is $T'(0) = -Q_h n_h^* \upsilon/\lambda$. Solving (42) with these initial conditions yields

$$T\left(x\right) = T_h + \frac{Q_h n_h^* \upsilon}{C_m\left(\upsilon_T - \upsilon\right)}\left(1 - \exp\left(\frac{C_m\left(\upsilon_T - \upsilon\right)x}{\lambda}\right)\right). \tag{43}$$

In particular, in the cracking region, $T = T_c$ and we find (19).

In a more detailed model of cracking, a distribution of various medium oil components must be considered. In this case the cracking region is wider. It is formed by thin cracking regions corresponding to all medium oil components, see Fig. 2 (thin dark interval is a cracking region for a specific component). Note that equations (18), (19), (42) and (43) do not contain the medium oil concentration n_c^*. This means that they can be used to compute the temperature and position of a cracking region for each medium oil component characterized by specific kinetic coefficients K_c and E_c.

Reaction-trailing structure

The HTO wave is assumed to be a traveling wave. The only reaction in this wave is oxidation. The gas flow is uniform in the HTO wave, $\rho u = \left(\rho u\right)_{inj}$. The heat balance in the wave is described by an equation similar to (39):

$$\upsilon Q_h(n_h^* - n_h^{unb}) + c_g\left(\rho u\right)_{inj}\left(T_i - T_h\right) = \upsilon C_m\left(T_i - T_h\right). \tag{44}$$

Using (37), we solve (44) for υ and obtain (21).

When the coke is not consumed completely in the HTO reaction, (37) yields the unburned coke concentration as (24). The condition $n_h^{unb} > 0$ gives $\upsilon > \left(\rho u Y\right)_{inj} M_h/n_h^*$. Substituting this inequality into (44) yields the lower bound (23).

Thermal wave

Cracking and vaporization are heat absorbing processes, which decrease the thermal wave speed compared to (9). The molar gas flux ahead of the wave is given by (25). The heat balance equation for this wave includes the heat rate $\upsilon_T\left(Q_c n_c^* + Q_v n_v^*\right)$ absorbed in cracking and vaporization, the heat $c_g\left(\rho u\right)_{inj}(T_h - T_{st}) - c_g\left(\rho u\right)_v(T_v - T_{st})$ transported by gas and the heat $\upsilon_T C_m\left(T_h - T_v\right)$ accumulated in the rock:

$$\upsilon_T\left(Q_c n_c^* + Q_v n_v^*\right) + \upsilon_T C_m\left(T_h - T_v\right) = c_g\left(\rho u\right)_{inj}(T_h - T_{st}) - c_g\left(\rho u\right)_v(T_v - T_{st}). \tag{45}$$

Using (25), we solve (45) as

$$\upsilon_T = \frac{c_g \left(\rho u\right)_{inj}}{C_m + C^*}, \quad C^* = \frac{Q_c n_c^* + Q_v n_v^*}{T_h - T_v}, \tag{46}$$

neglecting the small term $c_g (T_v - T_{st})\left(n_c^* / M_c + n_v^* / M_v\right)$ in the numerator of the second expression. In our model, the influence of cracking and vaporization given by the term C^* is usually small, so υ_T is close to the value in (9).